ELSEVIER

Study of cure kinetics of epoxy-silica organic–inorganic hybrid materials

J. Macan*, H. Ivanković, M. Ivanković, H.J. Mencer

Faculty of Chemical Engineering and Technology, University of Zagreb, Marulicev trg 19, p.p. 177, HR-10001 Zagreb, Croatia
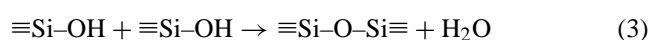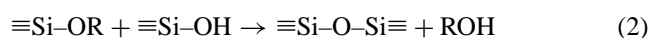
Abstract

Cure kinetics of organic–inorganic hybrids based on epoxy resin was investigated, using differential scanning calorimetry (DSC). Thermoset hybrid materials were prepared from diglycidyl ether of bisphenol A (DGEBA) as organic precursor, and 3-glycidyloxypropyltrimethoxysilane (GLYMO) as inorganic precursor. Precursors were polymerised simultaneously using poly(oxypropylene)diamine (Jeffamine D230) as a curing agent. Isothermal DSC characterisation of DGEBA/Jeffamine system and two hybrid DGEBA/GLYMO/Jeffamine systems, with DGEBA and GLYMO mixed in mass ratios of 2:1 and 1:1, respectively, was performed at different temperatures. Applicability of empirical models, commonly used to describe the curing kinetics of thermosets, to hybrid systems was investigated, and the resulting parameters were tested on dynamic DSC scans. Additionally, prepared materials were studied by FTIR and the extraction in tetrahydrofuran. The presence of inorganic phase was found to hinder complete cross-linking of organic phase and influence the kinetics of cure.
© 2004 Elsevier B.V. All rights reserved.

Keywords: Cure kinetics; Differential scanning calorimetry; Organic–inorganic hybrids; Sol–gel process

1. Introduction

Research of organic–inorganic hybrid materials, with inorganic phase dispersed on molecular or nano level in polymer matrix, has gained widespread attention in recent years. It is expected that increased interaction between phases in hybrid materials, where inorganic phase is often covalently bonded with the organic polymer, will result in superior properties compared to classical composites. Because of its flexibility and low reaction temperature, sol–gel process is often used to form nano-scale inorganic phase inside polymer matrix [1–8]. Inorganic phase is formed in situ by hydrolysis and condensation of metal (usually silicon) alkoxydes, as shown in following equations (R represents an alkyl group) [9]:

$$\equiv Si–OR + H_2O \Leftrightarrow \equiv Si–OH + ROH \qquad (1)$$

$$\equiv Si–OR + \equiv Si–OH \rightarrow \equiv Si–O–Si \equiv + ROH \qquad (2)$$

$$\equiv Si–OH + \equiv Si–OH \rightarrow \equiv Si–O–Si \equiv + H_2O \qquad (3)$$

Reactions of hydrolysis and condensation can be acid or base catalysed.

In this work, organic–inorganic hybrids based on an epoxy resin are prepared, with 3-glycidyloxypropyltrimethoxysilane (GLYMO) as the inorganic precursor. GLYMO is an organofunctional alkoxysilane monomer, and can undergo both the sol–gel polymerisation of the alkoxy groups as well as curing of the epoxy functionality to form a hybrid network containing covalent bonds between organic and inorganic phases. Several workers obtained hybrid materials based on epoxy resin using sol–gel process and reported their properties [7,10–18], but only Serier et al. [12,13] investigated cure kinetics of such materials. The goal of this work is to describe the cure kinetics of unmodified epoxy resin and of two hybrid systems by empirical models, and to determine the possible influence of sol–gel process and inorganic phase formation on kinetics of epoxy–amine reaction.

2. Experimental

2.1. Materials

An epoxy resin, diglycidyl ether of bisphenol A (DGEBA, Epikote 828 EL, Shell Chemicals) with the epoxy equivalent weight of 190 g/mol, and 3-glycidyloxypropyltrimethoxysilane (GLYMO, 98%, Aldrich, $M = 236$ g/mol) were used to synthesize organic–inorganic hybrid materials. Poly(oxypropylene) diamine (Jeffamine D230, Huntsman

---

* Corresponding author. Tel.: +385-1-4597-226; fax: +385-1-4597-250.

E-mail address: jmacan@pierre.fkit.hr (J. Macan).

Corporation) with N–H equivalent weight of 57.5 g/mol was used as a curing agent for epoxy groups, and as a basic catalyst of GLYMO hydrolysis. The materials were used as received.

2.2. Sample preparation

To prepare unmodified epoxy resin system, DGEBA and stoichiometric amount of Jeffamine were mixed and stirred at room temperature in a closed vessel for 90 min. To prepare hybrid materials, DGEBA and GLYMO were blended in weight ratios of 2:1 and 1:1 at room temperature in a closed vessel for 90 min. A stoichiometric amount of Jeffamine was added as a curing agent (30 phr for DGEBA and 23.8 phr for GLYMO). The mixtures were stirred for another 60 min. Hybrid materials were designated according to GLYMO:DGEBA weight ratios, as G1E2 (ratio 1:2) and G1E1 (ratio 1:1).

Samples for Soxhlet extraction and FTIR were cured for 24 h at room temperature, making use of air humidity for GLYMO hydrolysis, and then post-cured for 24 h at 120 °C in an oven.

2.3. Characterisation

The cure of investigated systems was studied by means of differential scanning calorimetry (DSC) on a Netzsch DSC 200 differential scanning calorimeter operating in the temperature range between −100 and 500 °C, using an empty aluminium pan as a reference. For isothermal experiments, sample was placed in the pre-heated DSC cell, and scan was started when the temperature equilibrium was regained. After the scan was completed, the sample was cooled to room temperature inside the DSC cell, and then reheated to 240 °C with a linear heating rate of 10 K min^{-1} in order to determine the residual heat of reaction. In non-isothermal experiments, sample was heated from room temperature to 240 °C, with linear heating rates of 1, 3, 5 and 10 K min^{-1}. The total heat of reaction, ΔH_T, is estimated from non-isothermal

experiments by drawing a straight line connecting the base line before and after the peak and integrating the area under the peak. Residual heat of reaction, ΔH_r, was determined in the same way, and the heat of isothermal reaction, ΔH_i, was estimated by extrapolating the final baseline.

Dynamic DSC experiments were also performed to determine the glass transition temperature, T_g, of the completely cured material. The sample was heated from room temperature to 250 °C at 10 K min^{-1}, then cooled in the DSC cell to 0 °C at 10 K min^{-1} and immediately reheated to 250 °C at 10 K min^{-1}. T_g was taken as the midpoint of the endothermic step transition.

FTIR spectra of pure ingredients and post-cured hybrid samples were obtained on a Nicolet Magna-IR 760 FT-IR. Each spectrum from 4000 to 600 cm^{-1} was averaged over 16 scans at resolution of 4 cm^{-1}. Liquid samples were coated on NaCl plates, while solid samples were mixed with dry KBr, ground into fine powder and pressed into pellets.

Soluble components of post-cured materials were extracted by Soxhlet extraction in refluxing tetrahydrofuran and characterised by FTIR.

3. Results and discussion

3.1. Reaction heats and the degree of conversion of epoxy groups

The total heats of reaction per mole of epoxy groups for all investigated systems, as well as glass transition temperatures and the percentage of soluble component are given in Table 1. The total heats of reaction for unmodified epoxy resin system determined both non-isothermally and isothermally are comparable. There is no residual activity since isothermal cure was performed at temperatures above T_g, and there is no influence of vitrification [19,20]. Although temperatures of isothermal cure for hybrid materials were also above their respective epoxy–amine network T_g, in those cases the residual activity was present.

Table 1
Heats of reaction per mole of epoxy groups determined by isothermal (ΔH_i, ΔH_r) and non-isothermal (ΔH_T) DSC characterisation, total conversion of epoxy groups, and glass transition temperature (T_g)

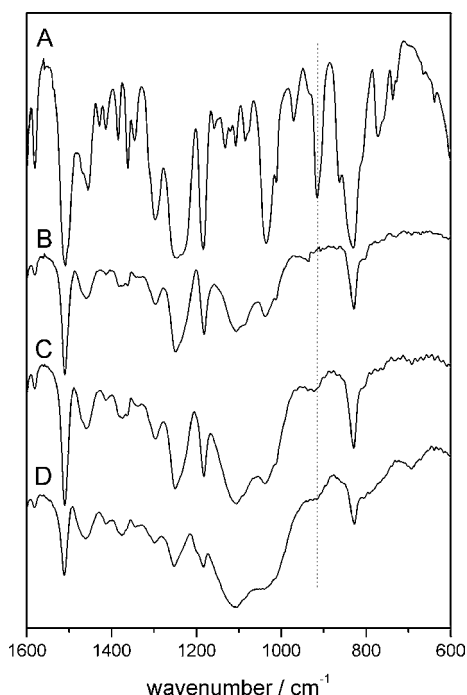| Material	T_i (K)	ΔH_i (kJ mol^{-1})	ΔH_r (kJ mol^{-1})	($\Delta H_i + \Delta H_r$) (kJ mol^{-1})	b (K min^{-1})	ΔH_T (kJ mol^{-1})	α_{tot}	T_g (K)
Epoxy	370	105	0	105 ± 1	5	106 ± 1	1.00	362
	375	104	0	104 ± 1	10	107 ± 2		
	380	105	0	105 ± 1				
G1E2	364	84	9	93 ± 9	1	92 ± 4	0.88	358
	369	82	1	83 ± 4	3	90 ± 4		
	374	80	2	82 ± 4	5	98 ± 4		
	379	76	3	79 ± 3	10	96 ± 3		
G1E1	369	84	5	89 ± 7	1	82 ± 4	0.81	355
	374	66	4	70 ± 6	3	89 ± 4		
	380	75	4	79 ± 5	5	92 ± 3		
	385	74	3	77 ± 4	10	80 ± 3		

Fig. 1. FTIR spectra: (A) DGEBA; (B) fully cured unmodified epoxy resin; (C) fully cured G1E2; (D) fully cured G1E1; dashed line represents the characteristic epoxide band at 916 cm^{-1}.

Fig. 2. Arrhenius plots of isothermal reaction rate constants for unmodified epoxy resin.

The value of 106 kJ/mol of epoxy groups obtained for unmodified epoxy resin system is in accordance with the value for epoxy–amine reaction found in literature [21] and indicates a complete conversion of epoxy groups. In hybrid materials, sol–gel reactions could also contribute to the total heat of reaction, but since no water was added and prepared mixtures were analysed immediately, it can be supposed that hydrolysis of GLYMO methoxy groups is slow compared to epoxy–amine reaction at higher temperatures [12,13], and therefore negligible. Preliminary investigation [22] showed that the molar heat of reaction of GLYMO epoxy ring with amine is the same as in DGEBA-amine systems. Equivalent heats per mole of epoxide were thus also determined from non-isothermal scans of hybrid materials, and the total conversion of epoxy groups, α_{tot}, was calculated, taking 106 kJ/mol epoxy as 100% conversion. Results are given in Table 1, and show decrease of epoxy groups conversion with the increasing content of inorganic phase.

This is confirmed by FTIR (Fig. 1), which shows that the characteristic epoxide band at 916 cm^{-1} disappears completely in fully cross-linked epoxy resin, but still remains to lesser extent in both hybrid materials. Soxhlet extraction of post-cured samples by tetrahydrofuran showed that only G1E1 contains 0.7% by weight of soluble component, identified by FTIR to be oligomer of DGEBA. This indicates that the inorganic phase is retained in the polymer matrix.

With increased content of inorganic phase, the glass transition shifts towards lower temperatures (Table 1), which is caused by plasticizing effect of products of GLYMO
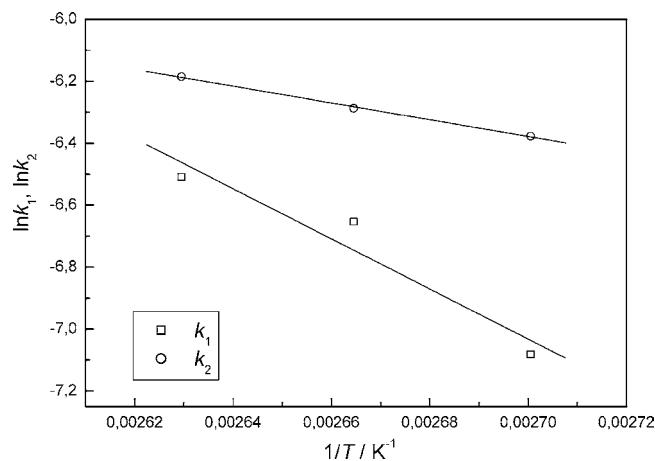
hydrolysis and condensation [15], as well as incomplete cross-linking of epoxy–amine organic matrix. All these results indicate that incomplete cross-linking in the hybrid systems is probably caused by sterical hindrances between the organic and inorganic component.

3.2. Cure kinetics for epoxy–amine system

In cure of epoxy resins with amine hardener, epoxy group can react either with primary or secondary amine. These reactions are catalysed by Lewis acids, phenols and alcohols. Thus the hydroxyl groups generated by amine are active catalysts, and the curing reaction shows an accelerating rate in its early stages, typical of autocatalysis [13].

The rate of reaction, $d\alpha/dt$, as a function of time was obtained from the rate of heat flow measured in isothermal DSC experiments, dH/dt, by:

$$\frac{d\alpha}{dt} = \frac{dH/dt}{\Delta H_T} \tag{4}$$

The average value of the total heat developed during non-isothermal DSC tests, ΔH_T, was taken as a measure of ultimate fractional conversion [23]. By partial integration of the area under $d\alpha/dt$ versus time curve, dependence of the fractional conversion, α, on time was obtained.

To describe cure kinetics, empirical model of Sourour and Kamal [24] was fitted to experimental data:

$$\frac{d\alpha}{dt} = (k_1 + k_2 \alpha^m)(1 - \alpha)^n \tag{5}$$

Parameters of the model (5), k_1, k_2, m and n, were determined from isothermal thermograms by Levenberg–Marquardt non-linear regression analysis (program Microcal Origin 6.0), under assumption that $m + n = 2$ [25,26]. Parameters m and n were found to be insensitive to temperature, and their average values were used in modelling. The temperature dependence of the apparent rate constants, k_1 and k_2, follows an Arrhenius relationship (Fig. 2):

Table 2
Parameters of the kinetic models (5) and (7) for listed systems

System	Model	Pre-exponential factor (s^{-1})	Activation energy $(kJ\,mol^{-1})$		m	n
Epoxy	(5)	k_{01} exp(14.8)	E_{a1}	67.2	0.58	1.42
		k_{02} exp(0.9)	E_{a2}	22.5		
G1E1	(7)	k_{01} exp(32.1)	E_{a1}	116.4		2.84
		k_{02} exp(10.5)	E_{a2}	53.6	0.19	1.63
G1E2	(7)	k_{01} exp(10.8)	E_{a1}	47.0		4.08
		k_{02} exp(15.8)	E_{a2}	68.8	0.20	1.80

$$k = k_0 \exp\left(\frac{-E_a}{RT}\right) \tag{6}$$

The parameters of the kinetic model (5) are summarised in Table 2.

To test the calculated parameters, differential Eq. (5) was solved numerically (program Wolfram Mathematica 4.1) for each temperature, as well as for non-isothermal conditions. Fig. 3. shows satisfying overlap of modelling results with
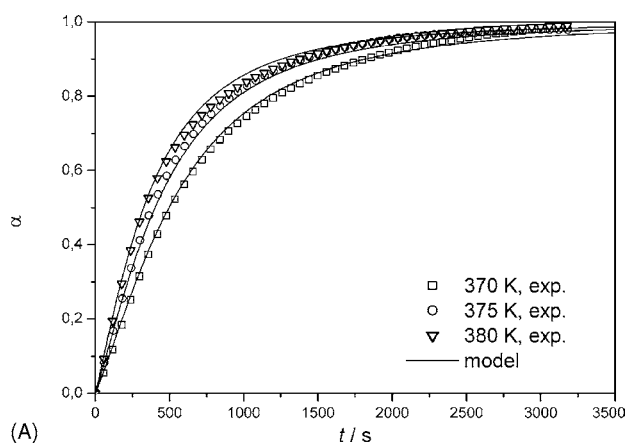
(A)
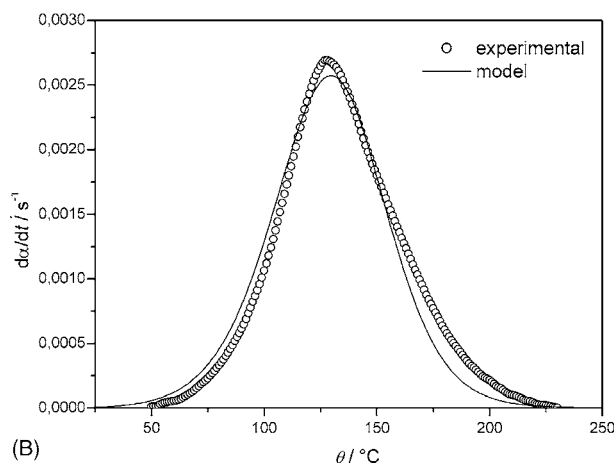
(B)

Fig. 3. Comparison of experimental data for unmodified epoxy resin with the kinetic model data: (A) isothermal fractional conversion as a function of time at reported temperatures; (B) non-isothermal reaction rate as a function of temperature at heating rate of $10\,K\,min^{-1}$.
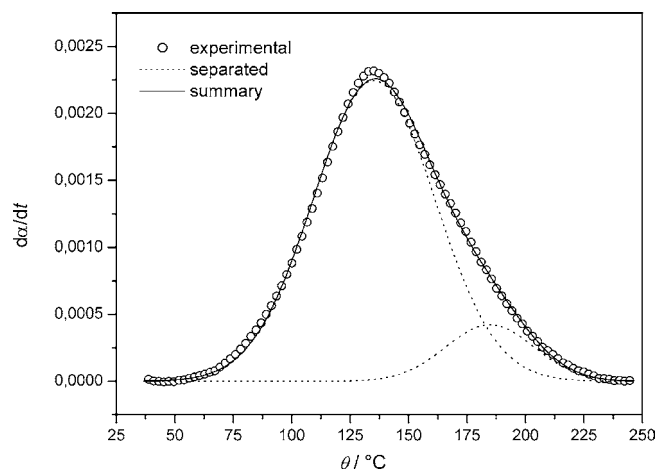

Fig. 4. Separation of the non-isothermal experimental reaction rate profile for G1E2 in contributions of two assumed reactions for illustration purposes; heating rate $10\,K\,min^{-1}$.

experimental data. Thus, a kinetic model with parameters determined by isothermal measurements performed in a relatively narrow temperature interval could be used to describe the dependence of reaction rate on temperature in non-isothermal conditions and for much wider temperature interval.

3.3. Cure kinetics for hybrid systems

Much larger scatter of experimental heat of reaction values obtained for hybrid materials in comparison with those of unmodified epoxy–amine system is probably the consequence of uncontrolled initial hydrolysis of GLYMO caused by the varying air humidity during the sample preparation. The total heats of reaction for G1E1 determined isothermally and non-isothermally are comparable (Table 1), with the notable exception of the value at 374 K. Therefore, $d\alpha/dt$ and α for the other three temperatures can be determined as described in Section 3.1. For G1E2, the average total heat of reaction determined isothermally is approximately 89% of the average non-isothermal total heat. Obviously asymmetrical shape of non-isothermal exothermic peak of G1E2 is indicative of a complex reaction. As an illustration, it can be separated into two Gaussian peaks representing simple reactions, the area of the first one being ∼88% of the total area of the peak (Fig. 4). Thus it can be presumed that isothermal characterisation of G1E2 only encompasses the reaction represented by the first non-isothermal exothermic peak, and so for this system the total heat of reaction as determined isothermally was taken to calculate $d\alpha/dt$ and α. Due to its anomalously low heat of reaction, the same procedure was applied to isothermal curve of G1E1 obtained at 374 K. Also, α_{tot} (Section 3.1) determined from the first non-isothermal peak of G1E2 is comparable with α_{tot} of G1E1. It can be presumed that in G1E2 organic chains, which are immobilised in inorganic structure, are able to react additionally at higher temperatures, while this
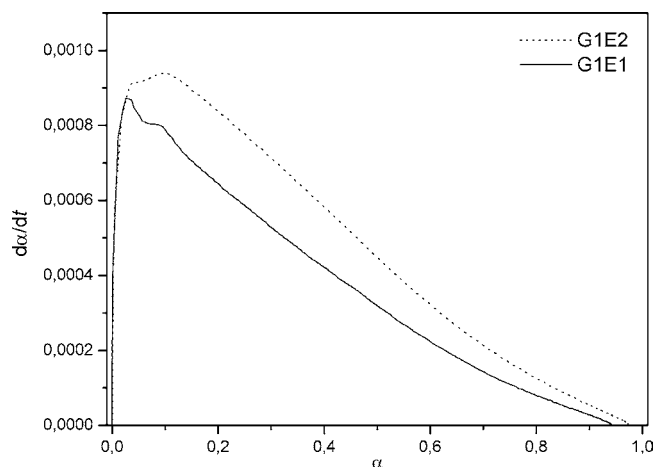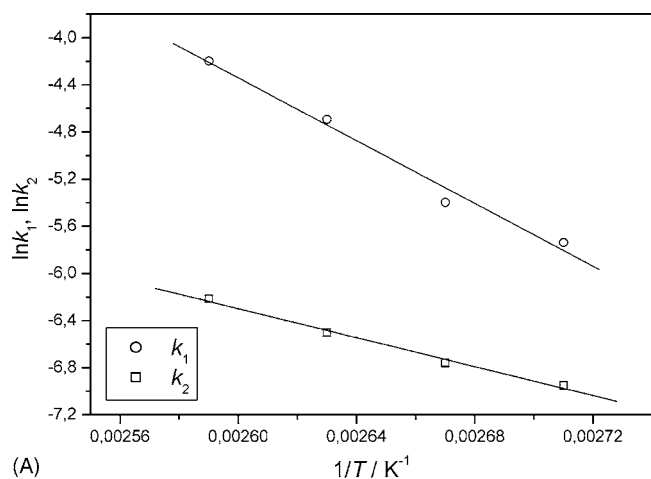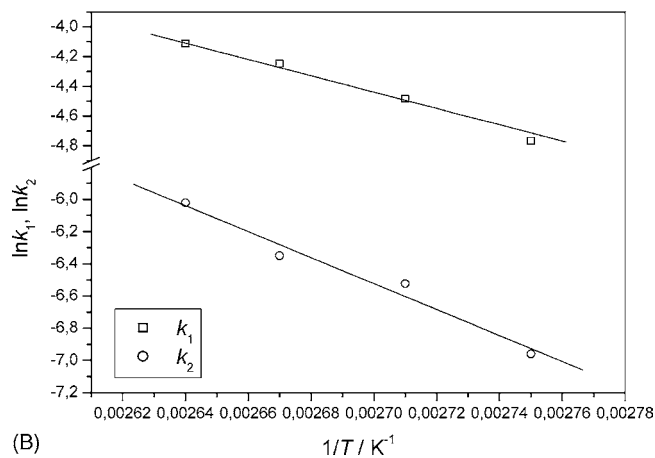
Fig. 5. Isothermal reaction rates at 374 K for investigated hybrid systems as functions of fractional conversion.

is impossible in G1E1 due to its higher content of inorganic phase. Because of the additional hindrance of cross-linked organic phase, this additional reactivity is not apparent in residual heats of reaction after isothermal cure of G1E2.
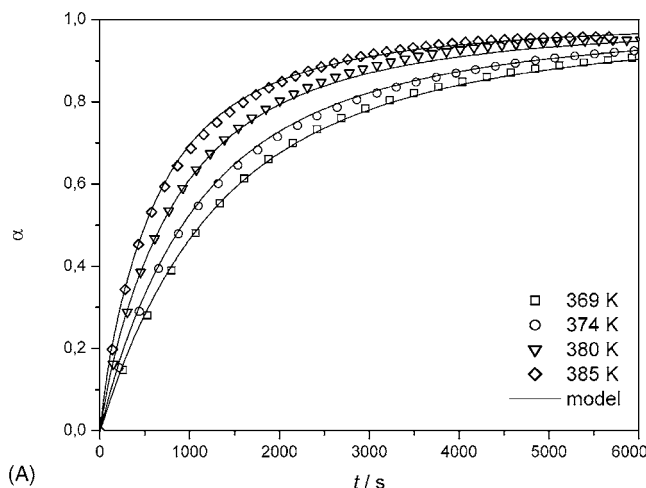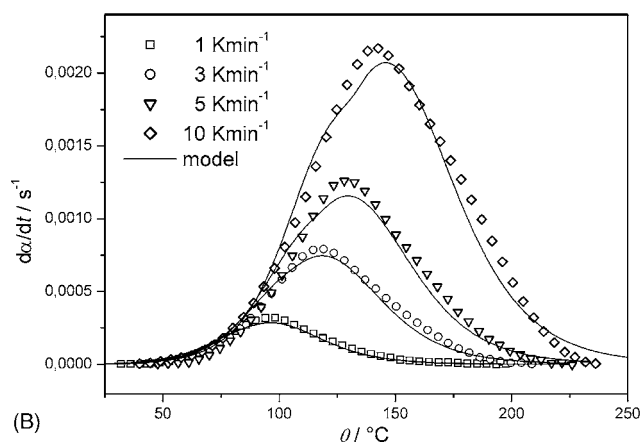

Fig. 6. Arrhenius plots of isothermal reaction rate constants for hybrid systems: (A) G1E1; (B) G1E2.

Fig. 7. Comparison of experimental data for hybrid system G1E1 with the kinetic model data: (A) isothermal fractional conversion as a function of time at reported temperatures; (B) non-isothermal reaction rate as a function of temperature at reported heating rates.

To choose an appropriate kinetic model, the shape of $d\alpha/dt$ versus time curve (Fig. 5) was studied. The existence of reaction rate maximum on the isothermal curve is characteristic for autocatalytic mechanism, but the shape of the curve indicates overlapping of such maximum with another reaction. It was found that this complex reaction can be adequately described by a sum of an autocatalytic model with an *n*-order model covering the conversion range $\alpha = 0.0$–0.4, which can tentatively be attributed to the influence of GLYMO on cure kinetics of epoxy groups. Thus, the following empirical model is proposed:

$$\frac{d\alpha}{dt} = k_1(0.4 - \alpha)^{n_1} + k_2\alpha^{m_2}(1 - \alpha)^{n_2} \tag{7}$$

The parameters of this model were determined as described (Section 3.2), and are listed in Table 2. Once more parameters n_1, m_2 and n_2 show no temperature dependence, while k_1 and k_2 follow an Arrhenius relationship (Fig. 6). Calculated parameters were also tested as described previously, and the results are shown in Figs. 7 and 8. The calculated parameters of the model provide satisfying description
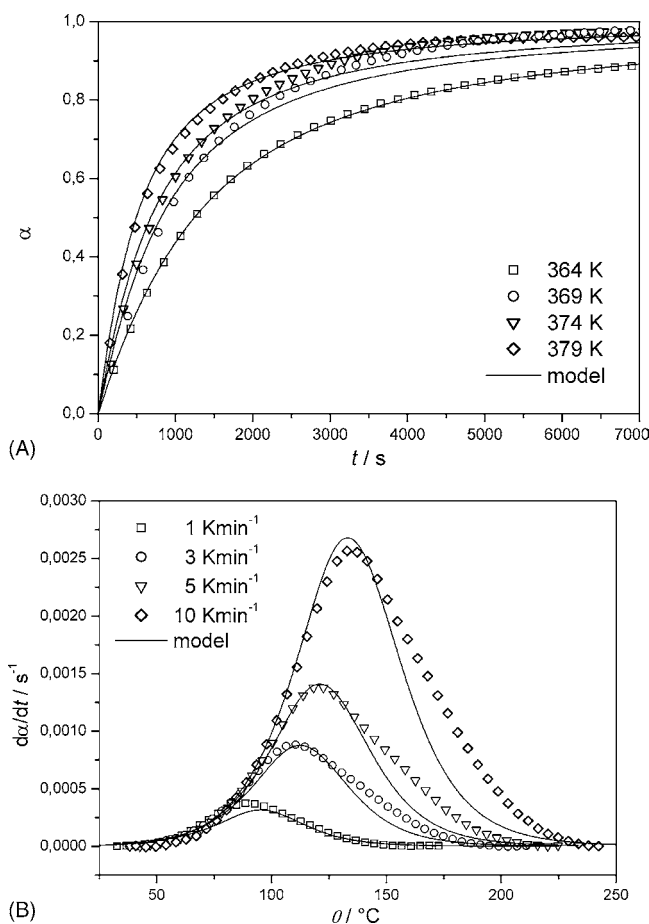
Fig. 8. Comparison of experimental data for hybrid system G1E2 with the kinetic model data: (A) isothermal fractional conversion as a function of time at reported temperatures; (B) non-isothermal reaction rate as a function of temperature at reported heating rates.

of isothermal reaction for system G1E1, and partially satisfying description for system G1E2. Cure kinetics in wide temperature interval and linear non-isothermal conditions are adequately described by model (7) for system G1E1, but for system G1E2 the model describes only the first exothermic peak. Due to limitations of the instrument [27] it is impossible to obtain valid isothermal measurements at higher temperatures, which correspond to the second reaction of G1E2. In the future work, it will be attempted to derive cure kinetics for this system from non-isothermal experiments [28]. Nonetheless, our proposed empirical model (7) can be useful in determining optimal conditions for cure and application of given epoxy-silica hybrid systems. Especially the good match of theoretical curves with independently obtained non-isothermal data confirms the validity of obtained kinetic parameters.

The first part of summary model (7) contributes significantly to the rate of reaction only at the very beginning (up to 30% conversion), and since the kinetics of only two hybrid systems were investigated, it is difficult to attribute physical meaning to the value of obtained parameters without further investigation. The parameters of the second part are compa-

rable to those of model (5). The sum $m_2 + n_2$ is 2 for G1E2 and 1.82 for G1E1. Activation energy, E_{a2}, is significantly lower for G1E1 compared to G1E2 and literature values for activation energy of epoxy–amine reactions [29]. This indicates possible catalytic influence of silanol groups, formed by hydrolysis of GLYMO and therefore present in greater number in the G1E1 hybrid material, on epoxy–amine reaction.

In investigated hybrid systems, sol–gel reactions of hydrolysis and condensation and sterical hindrances caused by formation of inorganic phase (Section 3.1) also influence cure kinetics of epoxy groups. This is contrary to work of Serier et al. [12,13], who investigated kinetics of epoxy reaction with aminosilane in solution, and found no influence of sol–gel reactions on kinetics of epoxy cure. Obviously, the determination of cure kinetics in bulk by empirical models takes into account not only chemical mechanism of the reaction, but also the effects of mass and heat transfer and chain mobility. Further investigations by complementary instrumental methods are necessary in order to fully clarify the cure mechanism of these hybrid materials.

4. Conclusions

The cure kinetics of pure DGEBA and two DGEBA–GLYMO hybrid materials (G1E1 and G1E2), with Jeffamine as hardener, was investigated by means of DSC, both isothermally at various temperatures and non-isothermally at various heating rates. Total conversion of epoxy groups was found to decrease with increasing content of GLYMO, which was confirmed by FTIR and Soxhlet extraction, and is attributed to sterical hindrance of inorganic phase. Reaction rate profiles were fitted to empirical models, which satisfactorily describe the reaction in wide temperature range up until complete conversion for unmodified epoxy resin and G1E1, and up to ~89% conversion for G1E2. Catalytic influence of silanol groups is indicated.

References

[1] M. Novak, Adv. Mater. 5 (1993) 422–433.
[2] E. Girard-Reydel, T.M. Lam, J.P. Pascault, Macromol. Chem. Phys. 195 (1994) 149–158.
[3] J.E. Mark, J. Appl. Polym. Sci. 58 (1995) 1135–1145.
[4] C.L. Jackson, B.J. Bauer, A.I. Nakatani, J.D. Barnes, Chem. Mater. 8 (1996) 727–733.
[5] J.E. Mark, Polymer 38 (1997) 4523–4529.
[6] D.W. McCarthy, J.E. Mark, D.W. Schaefer, J. Polym. Sci. Part B Polym. Phys. 36 (1998) 1167–1189.
[7] L. Matejka, O. Dukh, J. Kolarik, Polymer 41 (2000) 1449–1459.
[8] W. Zhou, J.E. Mark, M.R. Unroe, F.E. Arnold, J. Appl. Polym. Sci. 79 (2001) 2326–2330.
[9] R.C. Mehrotra, Present status and future potential of the sol–gel process, in: R. Reisfeld, C.K. Jørgensen (Eds.), Chemistry, Spectroscopy and Applications of Sol–Gel Glasses, Springer-Verlag, Berlin, 1992, pp. 1–36.

[10] L. Matejka, J. Pleštil, K. Dušek, J. Non-Cryst. Solids 226 (1998) 114–121.

[11] L. Matejka, K. Dušek, J. Pleštil, J. Kriz, F. Lednicky, Polymer 40 (1999) 171–181.

[12] A. Serier, J.P. Pascault, T.M. Lam, J. Polym. Sci. Part A Polym. Chem. 29 (1991) 209–218.

[13] A. Serier, J.P. Pascault, T.M. Lam, J. Polym. Sci. Part A Polym. Chem. 29 (1991) 1125–1131.

[14] A.N. Mauri, C.C. Riccardi, R.J.J. Williams, Macromol. Symp. 151 (2000) 331–340.

[15] L. Mascia, T. Tang, J. Sol–Gel Sci. Technol. 13 (1998) 405–408.

[16] V. Verganelakis, P.D. Nicolaou, C. Trapalis, G. Kordas, J. Non-Cryst. Solids 265 (2000) 265–275.

[17] M. Ochi, R. Takahashi, A. Terauchi, Polymer 42 (2001) 5151–5158.

[18] M. Ochi, R. Takahashi, J. Polym. Sci. Part B Polym. Phys. 39 (2001) 1071–1084.

[19] G. Wisanrakkit, J.K. Gillham, J. Appl. Polym. Sci. 41 (1990) 2885–2929.

[20] J. Enns, J.K. Gillham, J. Appl. Polym. Sci. 28 (1983) 2567–2591.

[21] J.M. Barton, The application of differential scanning calorimetry (DSC) to the study of epoxy resin curing reactions, in: K. Dusek (Ed.), Epoxy Resins and Composites. I. Advances in Polymer Science, vol. 72, Springer-Verlag, Berlin, 1985, pp. 112–154.

[22] J. Macan, H. Ivankovic, M. Ivankovic, H.J. Mencer, J. Appl. Poly. Sci., in press.

[23] J.M. Barton, Br. Polym. J. 11 (1979) 115–119.

[24] S. Sourour, M.R. Kamal, Thermochim. Acta 14 (1976) 41–59.

[25] J. Mijovic, J. Kim, J. Slaby, J. Appl. Polym. Sci. 29 (1984) 1449–1462.

[26] J. Mijović, J.D. Ott, J. Compos. Mater. 23 (1989) 163–194.

[27] J.M. Vergnaud, J. Bouzon, Cure of Thermosetting Resins: Modelling and Experiments, Springer-Verlag, Berlin, 1992.

[28] M. Maciejewski, Thermochim. Acta 355 (2000) 145–154.

[29] M.S. Lin, R.J. Chang, T. Yang, Y.F. Shih, J. Appl. Polym. Sci. 55 (1995) 1607–1617.